

Prefrontal CRF1-expressing neurons undergo enduring adaptations underlying aberrant emotional processing and alcohol drinking in abstinence

Reesha R. Patel¹, Sarah A. Wolfe¹, Vittoria Borgonetti¹, Shannon D'Ambrosio¹, Michal Bajo¹, Alain Domissy¹, Steven Head¹, Candice Contet¹, R. Dayne Mayfield², Amanda Roberts¹, and Marisa Roberto¹



¹Department of Molecular Medicine, The Scripps Research Institute, La Jolla, CA 92037; ²Department of Neuroscience, The University of Texas at Austin, Austin, TX 78712, USA

Introduction

Dysregulation of prefrontal circuits is thought to underlie aberrant emotional processing contributing to the persistent vulnerability to alcohol misuse in abstinence. Individuals with an alcohol use disorder (AUD) have reduced prefrontal volumes¹⁻³ and hypofunctionality of the medial prefrontal cortex (mPFC) contributes to loss of control over intake⁴. Preclinical studies also implicate the mPFC in anxiety-like behavior and excessive alcohol drinking⁵⁻⁶. **However, the discrete prefrontal cell-types and mechanisms underlying relapse remain largely unknown.**

Corticotropin-releasing factor (CRF) and its cognate type-1 receptor (CRF1) signaling, a prominent brain stress system, has been implicated in anxiety and AUD, particularly in limbic brain regions⁷⁻⁹. Little is known about CRF-CRF1 in prefrontal circuits in AUD. Functionally, mPFC injection of CRF or CRF antagonists has anxiogenic and anxiolytic effects, respectively⁹⁻¹², and deletion of forebrain CRF1 reduces anxiety¹³. Together, CRF1-expressing mPFC neurons (mPFC^{CRF1+}) respond to stress signals, that are dysregulated by chronic alcohol, and are wired to mediate anxiety; thus, mPFC^{CRF1+} are poised to mediate heightened anxiety-like behaviors promoting relapse in abstinence.

We tested the hypothesis that withdrawal from chronic alcohol uniquely impacts CRF1-expressing medial prefrontal cortex neurons underlying AUD-related behaviors contributing to relapse.

Identifying chronic alcohol-induced adaptations that persist into abstinence and drive aberrant behavior will provide insight into neuronal mechanisms for more efficacious therapeutic intervention, which are currently limited for AUD.

Methods

Animals: Adult male and female CRF1:GFP and CRF:Cre mice were used. All procedures were approved by Scripps Institutional Animal Care and Use Committee and were consistent with NIH Guidelines.

Chronic intermittent ethanol (CIE) inhalation model of alcohol dependence: Dependent mice received 16-hrs of ethanol vapor/day for 4 consecutive days each week for 5-6 weeks. Average blood ethanol levels during CIE were ~184mg/dl. Naive mice received air, and withdrawal mice were 5-8 days into forced abstinence from CIE inhalation.

Viral injections in the brain: Viruses (from Addgene or UNC vector core), indicated in the figures, were stereotactically injected into the basolateral amygdala (BLA; AP: -1.5, DV: -4.9, ML: 3.4) or the mPFC (AP: +1.9, DV: -2.4, ML: 0.05). Experiments were conducted after a minimum recovery period of 4 weeks.

In situ hybridization and immunohistochemistry: Phosphate-buffered saline and 4% paraformaldehyde perfused brains were cryoprotected in 30% sucrose and used for *in situ* hybridization using RNAscope according to the manufacturer's instructions or immunohistochemistry for staining with rabbit anti-CSF1 (Abcam).

Two-bottle 15% ethanol and water choice drinking (2-B): Following 3-4 weeks of baseline 2-B testing, consisting of 5 consecutive days of 2-hr 2-B sessions, CIE mice were interspersed with 2-5C weeks for 5-6 rounds of this 2-week cycle. To test effects of chemogenetic mPFC^{CRF1+} activation, i.p. injections of saline or 10mg/kg CNO (Tocris) were given 30 mins prior to 2-B testing during baseline and following 5-8 days of withdrawal from CIE.

Novelty-suppressed feeding test to measure anxiety-like behavior: Following 24 hrs of food deprivation, the latency to feed in a novel, open arena and then in the home cage were measured. Increased latency to feed in the open arena is indicative of increased anxiety-like behavior.

Ex vivo slice electrophysiology and optogenetic circuit dissection: Whole-cell voltage-clamp and current-clamp recordings were collected. A K-gluconate internal solution was used to record spontaneous excitatory postsynaptic potentials (eEPSCs) in artificial cerebrospinal fluid (ACSF), miniature excitatory postsynaptic potentials (mEPSCs) in the presence of 30μM bicuculline (BIC) and 0.5μM tetrodotoxin (TTX), and excitability in ACSF. Channelrhodopsin-2 (ChR2) elicited currents were measured using wide-field illumination (Sms, 493nm, 10mW) using a Cs-methanesulfonate internal solution and an external solution of ACSF containing 30μM BIC, 0.5μM TTX, and 100μM 4-aminopyridine.

Fluorescence activated cell sorting followed by RNA sequencing: The mPFC from naive and withdrawal CRF1:GFP mice were microdissected, live GFP+ cells were isolated with flow cytometry, RNA was isolated from GFP+ cells and sequenced. Transcripts were mapped to the mouse genome, differential gene analysis was performed, and gene network analysis was performed using AdvaTta.

Results

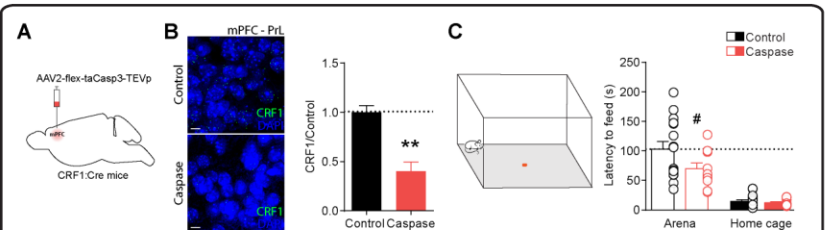


Figure 1. mPFC^{CRF1+} neurons regulate anxiety-like behavior.
A. Viral strategy to caspase-ablate mPFC^{CRF1+} neurons in CRF1:Cre mice. B. Representative *in situ* hybridization images depicting *Crtr1* (green) and DAPI (blue) expression in the mPFC of control (top) and caspase (bottom) mice. Quantification of *Crtr1* expressing neurons. *N* = 3 mice/group. ***p* < 0.01 by t-test. Scale bar = 10μm. C. Latency to feed in novelty-suppressed feeding test in an open arena and home cage in control and caspase mice with a significant main effects of location and group, and post hoc ***p* < 0.05 by two-way ANOVA. *N* = 10-15 mice/group.

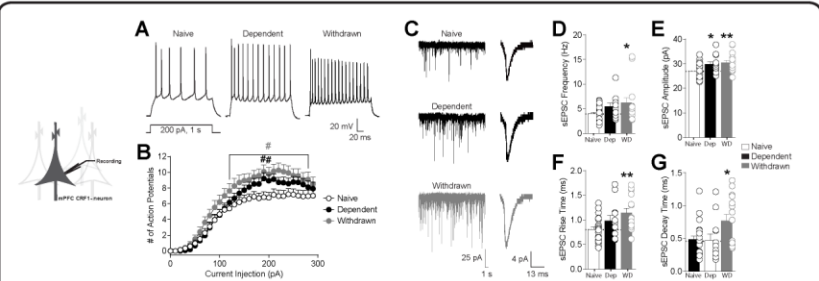


Figure 2. Ethanol dependence and withdrawal increase mPFC^{CRF1+} excitability and glutamate transmission.
A. Representative traces of excitability of mPFC prelimbic layer 2/3 CRF1 non-expressing (mPFC^{CRF1-}) neurons from naive, dependent, and withdrawal CRF1:GFP mice. B. Input-output curves. **p* < 0.05 and ***p* < 0.01 by post hoc analysis from two-way ANOVA. *n* = 24-35 cells from *N* = 6-10 mice. C. Representative traces of eEPSCs. D-G. eEPSC frequency, amplitude, rise time, and decay time, respectively. **p* < 0.05 and ***p* < 0.01 by one-way ANOVA. *n* = 12-22 cells from *N* = 6-10 mice.

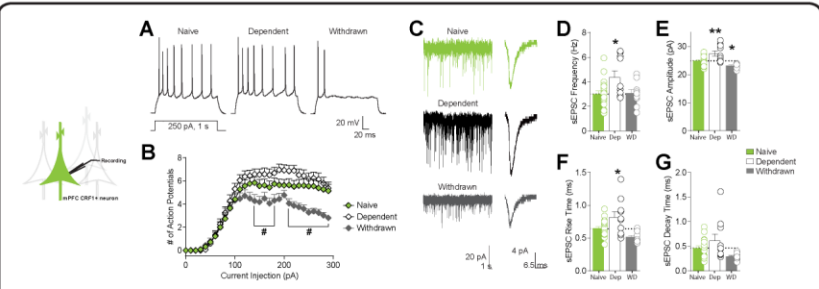


Figure 3. Ethanol withdrawal selectively decreases mPFC^{CRF1+} excitability and glutamate transmission.
A. Representative traces of excitability of mPFC^{CRF1+} prelimbic layer 2/3 neurons from naive, dependent, and withdrawal CRF1:GFP mice. B. Input-output curves. **p* < 0.05 by post hoc analysis from two-way ANOVA. *n* = 29-40 cells from *N* = 6-10 mice. C. Representative traces of eEPSCs. D-G. eEPSC frequency, amplitude, rise time, and decay time, respectively. **p* < 0.05 and ***p* < 0.01 by one-way ANOVA. *n* = 10-2 cells from *N* = 6-10 mice.

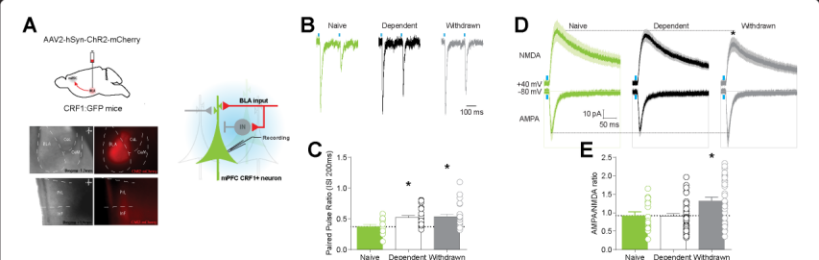


Figure 4. Ethanol dependence and withdrawal decreases glutamate release from basolateral amygdala inputs onto mPFC^{CRF1+} neurons contributing to the dysregulation of mPFC^{CRF1+} selectively in withdrawal.
A. DIC-IR and fluorescence images of viral injection site and BLA terminals in the mPFC. B-C. Representative traces and summary of paired pulse ratio measured in the BLA-mPFC^{CRF1+} pathway. D-E. Average traces of BLA-mediated NMDA and AMPA currents in mPFC^{CRF1+} cells and summary of AMPA/NMDA ratio. **p* < 0.01 by one-way ANOVA. *n* = 17-39 cells from *N* = 5-7 mice.

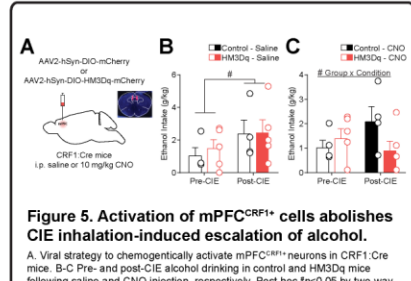


Figure 5. Activation of mPFC^{CRF1+} cells abolishes CIE inhalation-induced escalation of alcohol.
A. Viral strategy to chemogenetically activate mPFC^{CRF1+} neurons in CRF1:Cre mice. B-C. Pre- and post-CIE alcohol drinking in control and HMDQ mice following saline and CNO injection, respectively. Post hoc ***p* < 0.05 by two-way ANOVA. *N* = 9 mice.

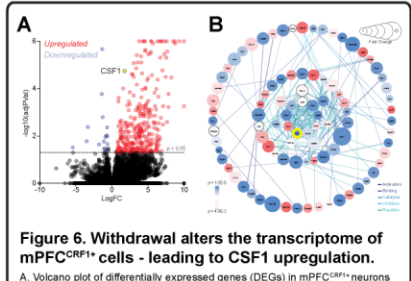


Figure 6. Withdrawal alters the transcriptome of mPFC^{CRF1+} cells - leading to CSF1 upregulation.
A. Volcano plot of differentially expressed genes (DEGs) in mPFC^{CRF1+} neurons from naive and withdrawal CRF1:GFP mice. B. Gene network analysis of DEGs, showing that colony-stimulating factor 1 (CSF1, in yellow) is a hub gene. *N* = 5-6 mice.

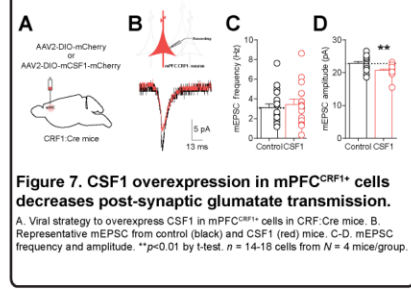


Figure 7. CSF1 overexpression in mPFC^{CRF1+} cells decreases post-synaptic glutamate transmission.
A. Viral strategy to overexpress CSF1 in mPFC^{CRF1+} cells in CRF:Cre mice. B. Representative mEPSC from control (black) and CSF1 (red) mice. C-D. mEPSC frequency and amplitude. ***p* < 0.01 by t-test. *n* = 14-18 cells from *N* = 4 mice/group.

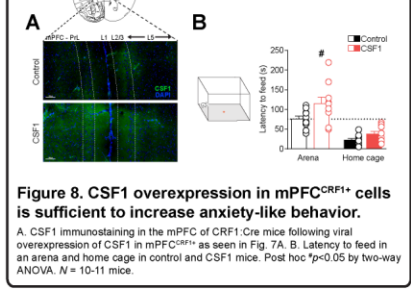


Figure 8. CSF1 overexpression in mPFC^{CRF1+} cells is sufficient to increase anxiety-like behavior.
A. CSF1 immunostaining in the mPFC of CRF1:Cre mice following viral overexpression of CSF1 in mPFC^{CRF1+}, as seen in Fig. 7A. B. Latency to feed in an arena and home cage in control and CSF1 mice. Post hoc *p* < 0.05 by two-way ANOVA. *N* = 10-11 mice.

Conclusions and Future Directions

- ▶ mPFC^{CRF1+} neurons regulate anxiety-like behavior and withdrawal-associated alcohol drinking, highlighting the potential role of this population in relapse during abstinence.
- ▶ mPFC^{CRF1+} neurons are selectively sensitive to withdrawal, and their dysregulation is driven in part by the BLA.
- ▶ Alcohol withdrawal alters the transcriptome of mPFC^{CRF1+} neurons - upregulating CSF1.
- ▶ Selective mPFC^{CRF1+} CSF1 overexpression mimics the observed synaptic neuroadaptations in mPFC^{CRF1+} neurons in withdrawal and heightens anxiety-like behavior, providing mechanistic insight into AUD-related behavior.
- ▶ Future studies will measure the impact of mPFC^{CRF1+} CSF1 in withdrawal-associated alcohol drinking.
- ▶ Future studies will identify discrete circuits comprising mPFC^{CRF1+} neurons and their role in AUD-related behavior.

Together, these findings highlight mPFC^{CRF1+} neurons as a critical site of enduring neuroimmune adaptations underlying aberrant behavior in withdrawal potentially contributing to relapse in AUD.

References and Acknowledgements

1. Jeromin TL, et al. Reduced cerebral grey matter observed in alcoholics using magnetic resonance imaging. *Alcohol Clin Exp Res*. 1991; 2. Pfefferbaum A, et al. Frontal lobe volume loss observed with magnetic resonance imaging in older chronic alcoholics. *Alcohol Clin Exp Res*. 1997; 3. Harris GU, et al. Frontal white matter and cingulum diffusion tensor imaging deficits in alcoholism. *Alcohol Clin Exp Res*. 2008; 4. Goldstein and Volkow. Dysfunctional prefrontal cortex in addiction: neuroimaging findings and clinical implications. *Nat Rev Neurosci*. 2011; 5. Fera and Durman. Prefrontal cortex circuits in depression and anxiety: contribution of discrete neuronal populations and target regions. *Mol Psychiatry*. 2020; 6. Klenowski PM. Emerging role for the medial prefrontal cortex in alcohol-seeking behaviors. *Addict Behav*. 2018; 7. Zornitzke EP, Longo ML, and Koob GF. Corticotropin releasing factor: a key role in the neurobiology of addiction. *Front Neuroendocrinol*. 2014; 8. Koob GF, et al. Addiction as a stress related disorder. *Neuropharmacology*. 2014; 9. Ikegami TT, Gomes KS, Nunes-de-Souza RL. Tonic modulation of anxiety-like behavior by CRF1 in the mPFC in male mice: role of PKA. *Hum Behav*. 2014; 10. Meloni EG, et al. Activation of raphe efferents to the mPFC by CRF: correlation with anxiety-like behavior. *Biol Psych*. 2008; 11. Jafar A and Bhargava S. CRF receptors in the mPFC regulate HPA activity and anxiety-related behavior regardless of prior stress experience. *Brain Res*. 2007; 12. Bilimova EY, et al. Local repeated CRF infusion exacerbates anxiety and fear-related behavior: differential involvement of the BLA and mPFC. *Neurosci*. 2011; 13. Refolo D, et al. Glutamatergic and dopaminergic neurons mediate anxiogenic and anxiolytic effects of CRF1. *Science*. 2011.

This work was supported by NIMHAAAA402149 (M.R.) and F32AA026765 (R.P.). We would like to thank the Scripps Animal Model, Flow Cytometry, Next Generation Sequencing, and the Computational Biology and Bioinformatics Core. Special thanks to Salvador Hator-Renzetti, Thom Potts, Stephanie E. Krause, Brian Seeger, Dr. Tony Mondala, Dr. Padma Narayan, Max Kreifeldt, Dr. Sohyun Lee, Dr. Kristin Baldwin, Dr. Larry S. Zweifel, and Dr. Wylie Vale for their various contributions to this project.